Multilevel regulation of bacterial gene expression with the combined STAR and antisense RNA system

Young Je Lee, Soo-Jung Kim and Tae Seok Moon*

Department of Energy, Environmental and Chemical Engineering, Washington University in St. Louis, St. Louis, MO, 63130, USA

* To whom correspondence should be addressed.

Tae Seok Moon

One Brookings Dr., Box 1180

St. Louis, MO 63130, USA

Tel: +1 (314) 935-5026

Fax: +1 (314) 935-7211

Email: tsmoon@wustl.edu

ABSTRACT

Synthetic small RNA regulators have emerged as a versatile tool to predictably control bacterial gene expression. Owing to their simple design principles, small size, and highly orthogonal behavior, these engineered genetic parts have been incorporated into genetic circuits. However, efforts to achieve more sophisticated cellular functions using RNA regulators have been hindered by our limited ability to integrate different RNA regulators into complex circuits. Here, we present a combined RNA regulatory system in *Escherichia coli* that uses small transcription activating RNA (STAR) and antisense RNA (asRNA) to activate or deactivate target gene expression in a programmable manner. Specifically, we demonstrated that the activated target output by the STAR system can be deactivated by expressing two different types of asRNAs: one binds to and sequesters the STAR regulator, affecting the transcription process, while the other binds to the target mRNA, affecting the translation process. We improved deactivation efficiencies (up to 96%) by optimizing each type of asRNA and then integrating the two optimized asRNAs into a single circuit. Furthermore, we demonstrated that the combined STAR and asRNA system can control gene expression in a reversible way and can regulate expression of a gene in the genome. Lastly, we constructed and simultaneously tested two A AND NOT B logic gates in the same cell to show sophisticated multi-gene regulation by the combined system. Our approach establishes a methodology for integrating multiple RNA regulators to rationally control multiple genes.

Keywords

Synthetic biology; RNA regulator; STAR; antisense RNA; genetic circuits

The ability to predictably and precisely control gene expression is a fundamental requirement for synthetic biologists to construct a genetic circuit that can reliably carry out real-world applications. To do so, a wide variety of genetic parts with tunable behaviors, simple design parameters, and a high degree of orthogonality should be developed and characterized. Of the many types of genetic parts that have been engineered, bacterial small RNAs (sRNAs) have proven to be effective and versatile in controlling gene expression.[1-3] sRNAs are found in nature, regulating many cellular processes such as iron homeostasis,[4] sugar metabolism,[5] and quorum sensing[6] in prokaryotes. Moreover, many engineered sRNAs or RNA regulators, including antisense RNAs (asRNAs),[7] small guide RNAs (sgRNAs),[8, 9] small transcription activating RNAs (STARs),[10, 11] riboswitches,[12] and toehold switches[13] have been developed to fine-tune bacterial gene expression in a programmable manner.[14]

RNA regulators have several potential advantages over protein regulators, including simple design principles,[15] highly orthogonal behavior,[16] and direct propagation of signals as RNAs.[17] Moreover, RNA regulators have relatively simple structures, which can be predicted by using software tools[18, 19] or experimentally verified by in-cell SHAPE-Seq[20] and probing system.[21] Owing to their versatility, RNA regulators are broadly utilized to engineer metabolic pathways,[22-24] construct genetic circuits,[10, 25, 26] and develop biosensors.[27] However, despite these advantages, few attempts have been made to integrate various RNA regulation mechanisms,[16, 28] which will ultimately enable the construction of complex genetic circuits with multi-input sensing and multi-gene regulation.[29] In our previous work, we constructed the combined CRISPR and asRNA system and developed design rules that describe the interaction between sgRNAs and asRNAs.[16] The combined CRISPR and asRNA system successfully controlled bacterial gene expression in *E. coli* (i.e. repression by the *Streptococcus pyogenes* dCas9-based CRISPR system and derepression by

the asRNA system). However, achieving activation and deactivation of bacterial gene expression by using the combined CRISPR and asRNA system would be challenging because the activation of gene expression using the CRISPR system has been demonstrated only in a host with a deletion of *rpoZ*, encoding ω subunit of RNA polymerase.[8] To address this bottleneck, this study demonstrated the use of two distinct types of RNA regulators, a STAR regulator and asRNA, in an integrated genetic circuit to activate and subsequently deactivate the target gene expression.

The STAR system has recently emerged as a powerful class of RNA regulators that can activate transcription of target genes, but its function with other bacterial sRNAs such as asRNA has not been fully explored. The STAR system consists of two different RNA elements: an intrinsic transcription terminator and a STAR regulator. The intrinsic transcription terminator or STAR-target is placed upstream of the coding region, which suppresses downstream transcription of target mRNA.[10] When a STAR regulator binds to a STAR-target through RNA-RNA interaction, it prevents the formation of the terminator hairpin and thus activates the target gene expression. Because the RNA-RNA interaction is sequence-specific, the STAR system can be highly orthogonal, potentially allowing for expression of multiple STAR regulators for multiplexed control of different genes. Furthermore, the STAR system has been characterized in a number of studies, making it a candidate for constructing an integrated genetic circuit.[30, 31]

Another well-studied class of RNA regulators used in this work is asRNA, which can finely control expression of target genes through sRNA-sRNA or sRNA-mRNA interactions.[7, 15, 16, 22] The sequence-specific RNA-RNA interaction can be facilitated by the native Hfq protein, an RNA chaperone protein that was proposed to protect asRNAs from degradation.[32-35] A synthetic asRNA can be designed by fusing a sequence that is complementary to its target RNA with an Hfq-binding RNA sequence.[2, 15, 22, 36] When asRNA-mRNA duplex forms through sequence-specific

interactions, translation and degradation rates are affected, mostly reducing the target gene expression level.[37] asRNA is an ideal candidate for engineering purpose as its design rules have been already determined.[15] Moreover, asRNA regulation has been previously used as an antagonistic regulator of sgRNA to dynamically derepress the target gene expression.[16]

The goal of this study is to simultaneously utilize two different RNA regulators that function by different mechanisms. Specifically, we seek to construct and characterize a genetic circuit that uses STAR regulators and asRNAs to control target gene expression in bacteria. The expression of the STAR regulator results in activation of target gene transcription, and subsequent expression of a *de novo* designed asRNA results in deactivation of target gene expression. To achieve deactivation of target gene expression, we pursued two strategies. The first approach requires the design of asRNAs that bind to and sequester STAR regulators (i.e. transcriptional control). The second approach utilizes asRNAs that bind to sequences around the ribosome binding site (RBS) and the start codon of the target mRNA (i.e. translational control). asRNAs used in this study were constructed following the design rules that have been determined.[15] The genetic parts, including an Hfq binding site, a target binding region (TBR) of asRNA, a transcription terminator of asRNA, and an origin of replication, were altered to not only improve the deactivation efficiency, but also understand the effect of genetic parts on the performance of the combined system. Next, we demonstrated the real-time control of target gene expression and showed expression control of a gene in the genome. Finally, we constructed two A AND NOT B logic gates in the same cell and demonstrated programmable expression control of two genes using two orthogonal STAR regulator-asRNA sets. This work demonstrates that RNA regulators are modular, and thus they can be functionally combined into complex genetic circuits to control multiple genes in a programmable manner.

RESULTS

STAR-mediated activation and asRNA-mediated deactivation of gene expression

A three-plasmid system was constructed to characterize the activation and deactivation of bacterial gene expression using the combined STAR and asRNA system (Figure 1). The first plasmid (ColE1 origin, high copy number) expresses green fluorescent protein (GFP) as a reporter. The second plasmid (R6K origin, variable copy number) transcribes a STAR regulator using the 3OC6-inducible P_{Lux} promoter. The last plasmid (ColE2 origin, variable copy number) transcribes either asSTAR or asGFP using the aTc-inducible P_{Tet} promoter. Unless stated otherwise, the three plasmid system was tested in *E. coli* JTK165JK (the strain in which plasmids with R6K or ColE2 origin are maintained at high copy numbers) to ensure that enough STAR regulators and asRNAs are transcribed.[38]

The activation of bacterial gene expression was first characterized using the STAR system only.[10] In the absence of the STAR regulator that acts as an anti-terminator, a STAR-target forms a terminator hairpin, which leads to rho-independent termination (Figures 1A and 1B). In the presence of the STAR regulator, the terminator hairpin of the STAR-target is disrupted, allowing for downstream transcription of the target gene. To select a STAR system with minimal basal expression and high fold-activation, four different STAR-targets (AD1.S5, STAR-target 1, STAR-target 2, and STAR-target 3) and three STAR regulators that bind to each STAR-target were tested by varying 3OC6 concentrations in the media (Supplementary Figure S1). The AD1.S5 STAR-target is a terminator from the pAD1 plasmid attenuation system, STAR-target 1 is a terminator from *Enterobacteria* phage λ, and STAR-targets 2 and 3 are both transcription terminators from

Registry of Standard Biological Parts (See Supplementary Table 2 for sequences).[39] Among the four STAR-targets tested, AD1.S5 demonstrated the lowest basal expression and the highest fold-activation when the AD1.A5 STAR regulator was used (13.8-fold without asSTAR and asGFP plasmids, Supplementary Figure S1A; 16.1-fold with the asSTAR plasmid, Figure 1C; 14.7-fold with the asGFP plasmid, Figure 1D). For subsequent experiments, the AD1.S5 STAR-target and the AD1.A5 STAR regulator were used to activate the GFP expression because they demonstrated the highest fold-activation with no growth defect in the range of 3OC6 concentrations tested (Supplementary Figures S2A and S2B).

We next sought two different approaches to achieve the deactivation of gene expression. The first approach requires the design of asRNAs that act as anti-anti-terminators. These asRNAs, which we denote as asSTARs, directly prevent STAR regulators from binding to STAR-targets (Figure 1A). An increase in asSTAR expression led to a decrease in GFP fluorescence levels without a growth defect (Figure 1E and Supplementary Figure S2C). We showed that up to 73.0% deactivation efficiency can be achieved with the optimized version of the combined system that includes the AD1.S5 STAR-target, AD1.A5 STAR regulator, and asAD1.A5 (the optimization process is described in detail below and shown in Figure 2). The second approach utilizes asRNAs that directly bind to sequences around RBS and the start codon of *gfpmut3* mRNA instead of STAR regulators (denoted as asGFP). The second approach achieves deactivation by preventing ribosomes from initiating translation (Figure 1B). An increase in asGFP expression led to a decrease in GFP fluorescence levels without a growth defect (Figure 1F and Supplementary Figure S2D). We observed up to 83.0% deactivation efficiency with the optimized version of the combined system that includes the AD1.S5 STAR-target, AD1.A5 STAR regulator, and asGFP1 (the optimization process is described in detail below and shown in Figure 2). To achieve the

highest deactivation efficiency, the STAR regulator and asSTAR or asGFP expressions were optimized by testing a range of 3OC6 and aTc concentrations. It was found that 5 μM 3OC6 and 100 ng/mL aTc resulted in the highest deactivation efficiency (73.0% for asAD1.A5 and 83.0% for asGFP1; Supplementary Figure S3).

In addition, we tested four control constructs in which a target binding region (TBR) is missing (no TBR control). TBR is a sequence of STAR regulators or asRNAs that is complementary to the target (i.e. STAR-target for activation; STAR regulator or *gfpmut3* mRNA for deactivation). These control plasmids contain no TBR under the control of the 3OC6-inducible P_{Lux} and aTc-inducible P_{Tet} promoters. All six combinations of plasmids were tested (named in the order of STAR-asRNA plasmids, including two experimental constructs): STAR-asSTAR; STAR-asGFP; no TBR-asSTAR; no TBR-asGFP; STAR-no TBR; and no TBR-no TBR. It was found that 3OC6 and aTc themselves did not affect GFP fluorescence in the range of concentrations tested (Supplementary Figure S5). More importantly, these no TBR control plasmids confirmed that activation and deactivation were due to sequence-specific RNA-RNA interaction.

Influences of genetic parts on deactivation efficiency

To study the influence of genetic parts on deactivation efficiency, we first designed asRNAs by fusing an Hfq binding site to a TBR sequence that is complementary to the target RNA (i.e. the AD1.A5 STAR regulator or *gfpmut3* mRNA) sequence.[22] We showed that the asRNAs with an Hfq binding site had higher deactivation efficiency than asRNAs without an Hfq binding site, determined by two-sample *t*-test (See Supplementary Figure S6 caption for the t- and p-values). Among different Hfq binding sites (MicC, Spot42, MicF M7.4, and MicF) that had been identified as high-performing sites in the literature[22, 36, 40], the MicF Hfq binding site was selected

because it showed the highest deactivation efficiency (Supplementary Figures S6). The MicF site was also found to have a low off-target effect.[15]

All asRNAs, except asAD1.A8 and asGFP7, were constructed following the asRNA design principles that we have determined in the previous report: ΔG Complex Formation value (less than -40 kcal/mol), double strand RNA length (greater than 15 nucleotides), and percent mismatch (less than 15%).[15] asAD1.A8 and asGFP7 were included as controls, which followed the design principles except their ΔG Complex Formation values that were greater than -40 kcal/mol (See Supplementary Figure S7 for the ΔG Complex Formation values of all asSTAR and asGFP variants). ΔG Complex Formation measures the binding free energy of the asSTAR-STAR regulator or asGFP-mRNA complexes, which was determined as previously described.[15] Several asSTARs (or asAD1 variants) that target the AD1.A5 STAR regulator were designed by varying the ΔG Complex Formation values (23-51 nucleotides and ΔG Complex Formation from -71.78 to -37.58 kcal/mol; Supplementary Figure S7). Of these, asAD1.A5 demonstrated the highest deactivation efficiency (45.4% before optimization; Figure 2A). Several asGFP variants that target *gfpmut3* mRNA were also designed by varying the ΔG Complex Formation values (20-38 nucleotides and ΔG Complex Formation from -74.78 to -33.98 kcal/mol; Supplementary Figure S7). Of these variants, asGFP1 showed the highest deactivation efficiency (46.0% before optimization; Figure 2A). A moderate negative correlation was observed between the ΔG Complex Formation and deactivation efficiency (i.e. the more negative the ΔG Complex Formation was, the higher deactivation efficiency was observed; Figure 2B).

Although the combined STAR and asRNA system functioned as expected, the deactivation efficiency on average was 26.3% (Figure 2A). Because the asRNAs were constructed following the design principles,[15] other genetic parts in the circuit such as the transcription terminators were

hypothesized to affect the deactivation efficiency. There are many native and synthetic bacterial transcription terminators that have been characterized and available for constructing genetic circuits.[41, 42] However, the extent of sequence diversity and the mechanistic variation cause transcription termination efficiency to vary.[43, 44] Additionally, the terminator sequence or structure itself might affect binding of asRNAs to their target RNA. Therefore, different transcription terminators may lead to different deactivation efficiencies. To test this hypothesis, six different transcription terminators were introduced on the 3'-end of asAD1.A5 and asGFP1 (the best performing asRNA from each category). Changes in the transcription terminator sequence resulted in a variation of deactivation efficiencies (Figure 2C). For example, while changing from se015 to B1002 terminator decreased the deactivation efficiency from 45.3% to 23.6% in the case of asAD1.A5, the same change increased the deactivation efficiency from 46.3% to 76.8% in the case of asGFP1. Despite the variation in the deactivation efficiencies, the K864501 terminator performed the worst, and the tracrRNA terminator from *Streptococcus pyogenes* performed the best for both asAD1.A5 and asGFP1 (Figure 2C).

To further improve the deactivation efficiency, the role of plasmid copy numbers was explored. Because the abundance of STAR regulators and asSTAR or asGFP depends on the plasmid copy number, the ratio of STAR regulators to asSTAR or asGFP can be varied by changing the copy number of plasmids. To vary the plasmid copy number, we utilized the genetically engineered *E. coli* strains (DIAL strains) bearing different alleles of *pir* and *repA* to support a wide range of copy numbers of plasmids containing the R6K and ColE2 origin.[38] The AD1.A5 STAR regulator and asAD1.A5 or asGFP1 were transcribed from the plasmids with the R6K and ColE2 origin, respectively. Various JTK165 DIAL strains (AK, EK, JB, JI, and JK) with different plasmid copy numbers were used to vary the levels of the AD1.A5 STAR regulators and

asAD1.A5 or asGFP1. The first and second letters denote the copy number of the R6K and ColE2 origin, respectively,[38] and represent the copy number in the order of low (A or B), medium (E or I), and high (J or K) (Figure 2D). The activation of *gfpmut3* expression increased as the copy number of the AD1.A5 STAR regulator plasmid increased (AK, EK, and JK strains). Likewise, the deactivation efficiency increased when the copy number of asAD1.A5 or asGFP1 plasmid increased (JB, JI, and JK strains).

Improved deactivation efficiency by integrating the two types of asRNAs

Next, we investigated the effect of utilizing both asSTAR and asGFP on deactivation efficiency. Because asSTAR and asGFP control the output gene expression at different levels (i.e. transcriptional and translational control, respectively), higher deactivation efficiency can be achieved by expressing both regulators. To test whether such multilevel gene regulation improves deactivation efficiency, each asRNA regulator was placed downstream of the aTc-inducible P_{Tet} promoter and upstream of the tracrRNA terminator, and both expression constructs were assembled on the same plasmid (ColE2 origin). This plasmid, along with two plasmids expressing either asSTAR or asGFP, was tested in JTK165JK strain (Figure 3). We observed an increase in deactivation efficiency from 70% or 81% (when either asAD1.A5 or asGFP1 was expressed) to 96% (when both asAD1.A5 and asGFP1 were used). A significant increase in deactivation was determined by two-sample *t*-test ($t = -10.11$, $p < 0.01$ when compared to asAD1.A5; $t = -5.18$, $p < 0.01$ when compared to asGFP1).

Real-time activation and deactivation of gene expression

One advantage of using the combined STAR and asRNA system is the fact that the gene expression control is reversible. Once the combined STAR and asRNA system had been

characterized and optimized, the ability to control gene expression in real time was tested using the AD1.A5 STAR regulator and asAD1.A5 or using the AD1.A5 STAR regulator and asGFP1. At time zero, cells with the combined system were induced with 5 μM 3OC6 to activate the STAR system only. The system responded within 4 h in cells with the asAD1.A5 plasmid (asAD1.A5 strain), determined by two-sample *t*-test ($t = 4.63$, $p < 0.05$; Figure 4A).[16, 45] On the other hand, the system responded within 5 h in cells with the asGFP1 plasmid (asGFP1 strain), determined by two-sample *t*-test ($t = 2.78$, $p < 0.01$; Figure 4B). The response is defined as a significant difference between the fluorescence levels of the negative control (uninduced cells) and the experimental strain (3OC6-induced cells). The long response time could be partially due to leakage of the aTc-inducible P_{Tet} promoter. Promoter leakage is defined as basal transcription of an uninduced promoter.[46] To further investigate the influence of promoter leakage on kinetics of GFP activation, we performed a kinetic experiment by inducing only the STAR system in cells that contain both the AD1.A5 STAR regulator and asRNA plasmids. Each asRNA plasmid contains asAD1.A5, asGFP1, or no TBR control placed downstream of the aTc-inducible P_{Tet} promoter. A significant gene activation was observed at 3 h (no TBR control), 4 h (asAD1.A5), and 5 h (asGFP1), determined by two-sample *t*-test ($t = 9.37$, $p < 0.05$ for no TBR control; $t = 4.63$, $p < 0.05$ for asAD1.A5; $t = 9.37$, $p < 0.01$ for asGFP1; Supplementary Figure S8). This result indicates that the delay in the response time is partially due to the leakage of the aTc-inducible P_{Tet} promoter (see the Discussion section for another reason).

The GFP expression reached its maximum level by 7 h (asAD1.A5 strain) and 9 h (asGFP1 strain), and the maximum fluorescence level was maintained for another 4 h. At 11 h (asAD1.A5 strain) and 13 h (asGFP1 strain), cells were diluted back to the initial absorbance of 0.01 by transferring cells into fresh media supplemented with both 5 μM 3OC6 and 100 ng/mL aTc to

maintain the STAR system and activate the asRNA system. The deactivation of *gfpmut3* expression was observed within 1 h, determined by two-sample *t*-test (t = 10.68, $p < 0.01$ for asAD1.A5 strain; $t = 2.78$, $p < 0.01$ for asGFP1 strain). This is the time point when the fluorescence level of the positive control (3OC6-induced cells) was significantly different from that of the experimental strain (3OC6- and aTc-induced cells). We found that the time by which the system responded (1 h) was independent of the duration of the activation tested (11 and 14 h for asAD1.A5 strain; 13 and 16 h for asGFP1 strain).

Regulation of a gene in the genome

The combined STAR and asRNA system can regulate the expression of a gene in the genome (Figures 5A and 5B). A cassette consisting of the Bba_J23119 constitutive promoter, AD1.S5 STAR-target, and *gfpmut3* was integrated into the JTK165JK genome (*bglA*::AD1.S5-*gfpmut3*) by expressing λ Red recombinase (see Supplementary Table 3 for the primers used).[47] The resulting *E. coli* strain possesses a functional copy of *gfpmut3* in the chromosome, but the transcription of the gene is repressed due to the AD1.S5 STAR-target. The AD1.A5 STAR regulator, asAD1.A5, and asGFP1 were transcribed from plasmids. We observed a 2.9-fold (asAD1.A5 strain; Figure 5C) and 2.6-fold (asGFP1 strain; Figure 5D) increase in the fluorescence level when the AD1.A5 STAR regulator was expressed. Next, we expressed asAD1.A5 or asGFP1 (5 μM 3OC6 and 100 ng/mL aTc) and observed deactivation efficiencies of 75.3% or 87.1%, respectively (Figures 5E and 5F). Because the STAR regulator in a plasmid would greatly outnumber the STAR-target (or *gfpmut3*) in the chromosome, the relatively low fold-activation would be expected (i.e. diminishing marginal returns when the STAR regulators are added to the already excess pool; Figure 5), compared to the fold-activation expected when *gfpmut3* is expressed on the plasmid (Figure 1). In other words, upon induction of STAR regulators, the low

number of the reporter gene (compared to that of STAR regulators) would limit the maximum 'on' expression level.

Relatively high basal expression of the STAR regulators (i.e. high STAR regulator-to-STAR-target ratio when the STAR-target (or *gfpmut3*) is expressed in the chromosome) can also amplify the effect of diminishing marginal returns on the fold-activation. Additionally, it was reported that a prerequisite for a STAR system to achieve high fold-activation is to minimize basal gene expression.[11] To access the contribution of basal expression to the low fold-activation, we performed a control experiment by measuring basal expression levels from six constructs (Supplementary Figure S9). Each STAR regulator plasmid contains either the AD1.A5 STAR regulator or no TBR control placed downstream of the 3OC6-inducible P_{Lux} promoter. Likewise, each asRNA plasmid contains asAD1.A5, asGFP1, or no TBR control placed downstream of the aTc-inducible P_{Tet} promoter. After testing all possible combinations, we found that P_{Lux} promoter leakage had an impact on the basal GFP fluorescence level (Supplementary Figure S9). The basal GFP fluorescence level increased by 67% due to the leaky expression of the AD1.A5 STAR regulator (P_{Lux} promoter leakage; Strain 5 vs. 6 in Supplementary Figure S9), and decreased by 52% due to the leaky expression of asGFP1 (P_{Tet} promoter leakage; Strain 4 vs. 6 in Supplementary Figure S9). However, when both STAR regulator and asRNA were present at the basal level, P_{Lux} promoter leakage, not P_{Tet} promoter leakage, had a dominating effect on the GFP level (82 and 52% increase for Strain 1 vs. 6 and 2 vs. 6, respectively).

Multilevel expression control of multiple genes

The activation and deactivation of multiple genes without crosstalk is another advantage of using the combined STAR and asRNA system. Here, we constructed two A AND NOT B logic gates (the output is 'on' only in the presence of A input and in the absence of B input), each of

which regulated either GFP or red fluorescent protein (RFP) expression in the same cell (Figure 6). First, a dual-color fluorescence reporter system was developed by inserting the AD1.S5 and STAR-target 2 upstream of the coding region of *gfpmut3* and *rfp*, respectively. Next, the target specificity of STAR regulators was tested by expressing the AD1.A5 or STAR2-1 STAR regulator in the same cell with the 3OC6-inducible P_{Lux} or IPTG-inducible P_{Lac} promoter. As expected, each STAR regulator only activated its target gene, but not affecting the non-target gene (Supplementary Figure S10A). Furthermore, the target specificity of asRNAs was tested by expressing asRNAs, along with the STAR regulators and both reporters, in the same cell. asAD1.A5 or asGFP1 was placed downstream of the aTc-inducible P_{Tet} promoter, and asSTAR2-1 or asRFP1 was placed downstream of the Ara-inducible P_{BAD} promoter. asAD1.A5 binds to the AD1.A5 STAR regulator, and asGFP1 binds to the *gfpmut3* mRNA to deactivate GFP expression. asSTAR2-1 binds to the STAR2-1 STAR regulator, and asRFP1 binds to the *rfp* mRNA to deactivate RFP expression. The results showed that all asRNAs deactivated their target gene expression only, while not affecting the non-target gene (Supplementary Figures S10B and S10C). These orthogonal sets of RNA regulators enabled construction of two A AND NOT B logic gates in the same cell, controlling two different genes in a programmable manner (Figure 6).

DISCUSSION

sRNAs that can regulate the transcription and translation of a target gene are commonly found in nature.[48-50] Based on these natural systems, various engineered RNA regulators that repress or activate the transcription or translation of target genes have been developed.[9, 10, 13, 25, 51, 52] Despite an increase in the number of engineered RNA regulators, a limited number of efforts have been made to integrate multiple engineered RNA regulators into a single system that achieves

multilevel gene regulation through direct RNA-RNA interaction in bacteria,[53, 54] let alone a multilevel gene regulatory system that consists of three different types of directly-interacting RNA regulators. Here, we showed that the STAR and asRNA systems can be combined to activate and subsequently deactivate a target gene expression through direct RNA-RNA interaction among three different types of regulators: STAR-target, STAR regulator, and asRNA. This new RNA-based gene regulation system is highly effective and reliable in regulating bacterial gene expression in a programmable manner (Figures 1-6). The work described here will further expand our ability to integrate multiple RNA regulators and control expression of multiple genes to achieve complex cellular behavior (Figure 6).

The combined STAR and asRNA system was constructed by integrating two different RNA regulators into a single system (Figures 1 and 2). First, the STAR regulator was designed to target the STAR-target that was placed upstream of the coding region. Upon binding of the STAR regulator to the STAR-target, the terminator hairpin structure is disrupted, activating the transcription of the downstream gene. Next, two different types of asRNAs were designed to deactivate target gene expression: the asSTAR that targets the STAR regulator, and asGFP that targets the mRNA. While the STAR-targeting deactivation was achieved at the transcriptional level, the mRNA-targeting deactivation was achieved at the translational level. Our results showed that deactivation efficiency of 73.0% can be achieved when asAD1.A5 binds to the AD1.A5 STAR regulator and that deactivation efficiency of 83.0% can be achieved when asGFP1 binds to the *gfpmut3* mRNA (Figure 1). To further enhance the deactivation efficiency, we simultaneously expressed asSTAR and asGFP to regulate the reporter gene at both transcriptional and translational levels, which resulted in 96% deactivation efficiency (Figure 3). This is an example of utilizing

three different types of sRNAs (STAR regulator, asSTAR, and asGFP) that function at different control points to effectively regulate gene expression.

One of the advantages of using the combined STAR and asRNA system is that gene expression can be reversibly controlled (Figure 4). The real-time control of gene expression could particularly be useful in controlling the flux of metabolic pathways. In metabolic engineering, introduction of heterologous genes often leads to a flux imbalance and metabolic burdens that result in low productivity.[55-57] To address this problem, metabolic engineers regulate expression of heterologous genes by changing the strength of promoters and RBSs.[22] However, optimizing the expression level of individual enzymes with different promoters and RBSs is labor-intensive. The combined STAR and asRNA system might offer an alternative approach to address the flux imbalance problem by fine-tuning the expression of enzymes at different time points. While studying the kinetics of the combined STAR and asRNA system, we observed that the leakage of the P_{Tet} promoter (i.e. basal asRNA expression) affected the response time of output gene activation (3 h for no TBR control, 4 h for asAD1.A5, and 5 h for asGFP1; Supplementary Figure S8). Thus, utilizing promoters with low leakage to minimize the basal expression of asRNAs would lead to fast gene activation. Furthermore, our data indicates that deactivation occurred quickly (i.e. the decrease in the fluorescence level was observed within 1 h; Figure 4). Because GFP protein is stable, the rate of decrease in the fluorescence level is most likely determined by protein dilution due to cell growth.[9, 58] It is worth noting that asRNAs are quickly produced through the transcription process and interact quickly with their target for deactivation, compared to the slower activation process that requires transcription of a sufficient number of STAR regulators in the presence of basal levels of asRNAs, followed by both transcription and translation of GFP.

A key limitation in constructing genetic circuits that implement complex cellular functions

is the limited number of orthogonal parts. Here, we constructed four A AND NOT B logic gates using four orthogonal sets of the combined STAR and asRNA system to regulate expression of multiple genes (Figure 6 and Supplementary Figure S10). We showed that multiple orthogonal RNA regulators can be designed and constructed to specifically activate and deactivate particular gene expression.

In synthetic biology, the first genetic circuits were constructed by utilizing a small number of protein regulators.[59, 60] Since these pioneering reports, various protein regulators have been put together to construct simple to complex genetic circuits, exploring the dynamic circuit functions.[61-64] In addition to protein regulators, RNA regulators have been extensively engineered and utilized in construction of genetic circuits due to their simple design principles and highly orthogonal behavior.[65-67] In an attempt to understand ways to integrate various RNA regulators with independent mechanisms of action, we combined STAR and asRNA systems to activate and subsequently deactivate expression of multiple genes. The versatility of the combined STAR and asRNA system suggests that more complex integration of diverse RNA regulators is possible in the future to implement complex cellular functions.

METHODS

Strains and culture media

E. coli JTK165JK DIAL strain was used for all the experiments to maintain high copy numbers of plasmids expressing STAR regulators (variable R6K origin of replication) and asRNAs (variable ColE2 origin of replication).[38] Other JTK165 variants (JTK165AK, EK, JB, and JI) were also used to test the effect of changing the plasmid copy number on deactivation efficiency (Figure

2D). All plasmid constructions were performed in *E. coli* DH10B[68] or JTK165JK[38] depending on the origin of replication of the plasmid (ColE1 or p15A in DH10B; and R6K or ColE2 in JTK165JK). Cells were grown in LB media (10 g/L tryptone, 10 g/L NaCl, and 5 g/L yeast extract) supplemented with the appropriate antibiotics: ampicillin (100 μg/mL), kanamycin (20 μg/mL), spectinomycin (100 μg/mL), and chloramphenicol (34 μg/mL). Inducers were used at the following concentrations: 3OC6 (3-oxohexanoyl-homoserine lactone, 0-20 μM), aTc (anhydrotetracycline, 0-100 ng/mL), IPTG (isopropyl β-D-1-thiogalactopyranoside, 20 mM), and Ara (arabinose, 40 mM). All chemical reagents and inducers used in this study were from Sigma-Aldrich (St. Louis, MO, USA).

Plasmid construction and genetic circuit design

The RNA regulator sequences were inserted into plasmids using synthetic oligonucleotides (Integrated DNA Technologies, Coralville, IA, USA) and Phusion High-Fidelity DNA polymerase (New England Biolabs, Ipswich, MA) through inverse PCR (See Supplementary Table 1 for all constructed plasmids and Supplementary Table 2 for RNA regulator sequences). The amplified and purified DNA fragments were simultaneously phosphorylated with T4 polynucleotide kinase (New England Biolabs, Ipswich, MA) and ligated with T4 DNA ligase (New England Biolabs, Ipswich, MA) at room temperature for 1 h. Electrocompetent *E. coli* DH10B or JTK165JK was transformed with the ligated DNA products (Eppendorf Eporator). The transformants were grown on LB agar plate with appropriate antibiotics (overnight at 37°C). Constructed plasmid sequences were verified by DNA sequencing (PNACL, Washington University School of Medicine). Plasmids were purified from the overnight culture using a miniprep kit (Zymo Research, Irvine, CA) and stored at -20°C for the future usage. All other necessary genetic parts (origin of replication, promoters, terminators, RBS, and reporter genes) used in this study were combined by the Golden-

Gate DNA assembly technique using either BspMI (New England Biolabs, Ipswich, MA) or AarI Type IIS restriction enzymes (Thermo Fisher Scientific, St. Peters, MO).[69]

Two different types of RNA regulators (STAR regulator and asRNA) were designed and used for the experiments. First, the complementary sequences of STAR-targets were used to design STAR regulators. The pheA-1 transcription terminator was inserted on the 3'-end of the STAR regulators.[44] Next, asSTAR and asGFP were designed by using a sequence that is complementary to the target RNA (the AD1.A5 STAR regulator for asSTAR and *gfpmut3* mRNA for asGFP) sequences. The target region was restricted to 68 nucleotides of the AD1.A5 STAR regulator, or 80 nucleotides containing the RBS (-16 to +64 with the start codon's A as +1) of *gfpmut3* mRNA. asSTARs and asGFPs were constructed following the asRNA design principles: ΔG Complex Formation value (less than -40 kcal/mol), double strand RNA length (greater than 15 nucleotides), and percent mismatch (less than 15%).[15] The ΔG Complex Formation of asSTAR-STAR regulator or asGFP-*gfpmut3* mRNA was calculated using the NUPACK software package.[18] The sequences of all genetic parts used in this work are shown in Supplementary Table 2.

Integration of genetic parts into the *E. coli* genome

Integration of genetic parts into the *E. coli* genome was done according to the reported method with some modification.[47] Briefly, the AD1.S5-*gfpmut3* cassette consisting of the constitutive BBa_J23119 promoter, AD1.S5 STAR-target, RBS, and *gfpmut3* was integrated into the *E. coli* JTK165JK chromosome in the middle of the *bglA* gene. The kanamycin-resistant gene and FLP recognition target (FRT) sites were amplified from pKD13 using the bglA1F/bglA1R primer set (Supplementary Table 3). The AD1.S5-*gfpmut3* cassette was amplified from the pRL01 plasmid (Supplementary Tables 1 and 2) using the bglA2F/bglA2R primer set (Supplementary Table 3). Both PCR-amplified DNA fragments were fused by the overlap extension PCR. The

JTK165JK cells harboring the pKD46 plasmid were grown for 2 h in 5 mL LB media with 100 μg/mL ampicillin and 10 mM arabinose at 30°C (250 rpm), and the cells were prepped for electroporation. The arabinose induces the λ Red recombinase expression. The electrocompetent JTK165JK cells were transformed with 100 ng of the overlap extension PCR product and grown overnight (approximately 16 h) on LB/kanamycin agar plate at 37°C. pKD46 plasmid was cured during the cultivation on the plate at 37°C. The kanamycin-resistant gene in the genome was removed by expressing FLP recombinase from the pCP20 plasmid. The pCP20 plasmid was cured by culturing the cell for 12–16 h in 5 mL LB media without ampicillin at 37°C, resulting in the JTK165JK-AD1.S5-*gfpmut3* strain (Figure 5).

Fluorimetry

Cells were grown overnight in 5 mL LB media with appropriate antibiotics at 37°C and 250 rpm (New Brunswick Excella E25 shaking incubator). The overnight cultures were subcultured (1% v/v) in fresh 5 mL LB media with appropriate antibiotics and grown for 2 h at 37°C and 250 rpm. The subcultures were transferred to fresh 0.6 mL LB media, supplemented with appropriate antibiotics and inducers (at concentrations as indicated in figure captions), in deep 96-well plates (Eppendorf, Hamburg, Germany). The transferred cells were grown for 21 h at 37°C and 250 rpm, and centrifuged to form a cell pellet. The cell pellets were resuspended in 0.2 mL phosphate-buffered saline (pH 8.0) and the population fluorescence was measured using a Tecan microplate reader (Infinite M200 Pro). The background fluorescence value of phosphate buffered saline was subtracted from the measured sample fluorescence, and then this corrected value (F) was normalized by dividing it by the absorbance measured at 600 nm (Abs). The deactivation efficiency was calculated by $[(F_{STAR}/Abs_{STAR} - F_{STAR,asRNA}/Abs_{STAR,asRNA}) / (F_{STAR}/Abs_{STAR} - F_{negative\ control}/Abs_{negative\ control})] \times 100\%$, where the subscript indicates induced systems and the

negative control is JTK165JK with both STAR and asRNA systems uninduced. The GFP fluorescence was measured with excitation at 483 nm and emission at 530 nm. The RFP fluorescence was measured with excitation at 535 nm and emission at 620 nm.

Flow cytometry

Cells were grown overnight in 5 mL LB media with appropriate antibiotics at 37°C and 250 rpm. The overnight cultures were transferred to fresh 0.6 mL LB media (Abs = 0.01), supplemented with appropriate antibiotics and 5 μM 3OC6, in a deep 96-well plate, and grown for the indicated hours at 37°C and 250 rpm (Figure 4). The cells were collected every hour and transferred to 200 μL filtered 0.9% (w/v) saline (pH8.0) to measure the fluorescence using a Millipore Guava EasyCyte High Throughput flow cytometer (a 488 nm excitation laser and 512/18 nm emission filter). After 11 or 14 h for asAD1.A5 and 13 or 16 h for asGFP1, the GFP activated cells were transferred into fresh LB media (Abs = 0.01) with appropriate antibiotics and inducers (5 μM 3OC6 and 100 ng/mL aTc) and grown for indicated hours at 37°C and 250 rpm (Figure 4). All the cytometry data were gated by forward and side scatter, and each data was obtained from at least 5000 gated cells. FlowJo (TreeStar Inc.) was used to obtain the arithmetic mean of each fluorescence distribution.

SUPPORTING INFORMATION

Supplementary Figures S1-S10 and Supplementary Tables 1-3 are available.

ACKNOWLEDGEMENT

We thank Charles Johnson for his initial work and Drew DeLorenzo for helpful comments on the manuscript. This work was supported by the National Science Foundation (CBET-1350498 and MCB-1714352).

CONFLICT OF INTEREST

The authors declare no conflict of interest.

REFERENCES

[1] Lucks, J. B., Qi, L., Mutalik, V. K., Wang, D., and Arkin, A. P. (2011) Versatile RNA-sensing transcriptional regulators for engineering genetic networks, *Proc. Natl. Acad. Sci. U.S.A. 108*, 8617-8622.
[2] Yoo, S. M., Na, D., and Lee, S. Y. (2013) Design and use of synthetic regulatory small RNAs to control gene expression in *Escherichia coli*, *Nat. Protoc. 8*, 1694-1707.
[3] Lahiry, A., Stimple, S. D., Wood, D. W., and Lease, R. A. (2017) Retargeting a Dual-Acting sRNA for Multiple mRNA Transcript Regulation, *ACS Synth. Biol. 6*, 648-658.
[4] Masse, E., and Gottesman, S. (2002) A small RNA regulates the expression of genes involved in iron metabolism in *Escherichia coli*, *Proc. Natl. Acad. Sci. U.S.A. 99*, 4620-4625.
[5] Bobrovskyy, M., and Vanderpool, C. K. (2014) The small RNA SgrS: roles in metabolism and pathogenesis of enteric bacteria, *Front. Cell. Infect. Microbiol. 4*, 61.
[6] Lenz, D. H., Mok, K. C., Lilley, B. N., Kulkarni, R. V., Wingreen, N. S., and Bassler, B. L. (2004) The small RNA chaperone Hfq and multiple small RNAs control quorum sensing in *Vibrio harveyi* and *Vibrio cholerae*, *Cell 118*, 69-82.
[7] Man, S. A., Cheng, R. B., Miao, C. C., Gong, Q. H., Gu, Y. C., Lu, X. Z., Han, F., and Yu, W. G. (2011) Artificial trans-encoded small non-coding RNAs specifically silence the selected gene expression in bacteria, *Nucleic Acids Res. 39*, e50.
[8] Bikard, D., Jiang, W. Y., Samai, P., Hochschild, A., Zhang, F., and Marraffini, L. A. (2013) Programmable repression and activation of bacterial gene expression using an engineered CRISPR-Cas system, *Nucleic Acids Res. 41*, 7429-7437.
[9] Qi, L. S., Larson, M. H., Gilbert, L. A., Doudna, J. A., Weissman, J. S., Arkin, A. P., and Lim, W. A. (2013) Repurposing CRISPR as an RNA-guided platform for sequence-specific control of gene expression, *Cell 152*, 1173-1183.
[10] Chappell, J., Takahashi, M. K., and Lucks, J. B. (2015) Creating small transcription activating RNAs, *Nat. Chem. Biol. 11*, 214-220.
[11] Chappell, J., Westbrook, A. M., Verosloff, M., and Lucks, J. B. (2017) Computational design of small transcription activating RNAs for versatile and dynamic gene regulation, *Nat. Commun. 8*, 1051.
[12] Win, M. N., and Smolke, C. D. (2007) A modular and extensible RNA-based gene-regulatory platform for engineering cellular function, *Proc. Natl. Acad. Sci. U.S.A. 104*, 14283-14288.
[13] Green, A. A., Silver, P. A., Collins, J. J., and Yin, P. (2014) Toehold switches: de-novo-designed regulators of gene expression, *Cell 159*, 925-939.
[14] Lee, Y. J., and Moon, T. S. (2018) Design rules of synthetic non-coding RNAs in bacteria, *Methods*. https://doi.org/10.1016/j.ymeth.2018.01.001

[15] Hoynes-O'Connor, A., and Moon, T. S. (2016) Development of Design Rules for Reliable Antisense RNA Behavior in *E. coli*, *ACS Synth. Biol. 5*, 1441-1454.
[16] Lee, Y. J., Hoynes-O'Connor, A., Leong, M. C., and Moon, T. S. (2016) Programmable control of bacterial gene expression with the combined CRISPR and antisense RNA system, *Nucleic Acids Res. 44*, 2462-2473.
[17] Takahashi, M. K., Chappell, J., Hayes, C. A., Sun, Z. Z., Kim, J., Singhal, V., Spring, K. J., Al-Khabouri, S., Fall, C. P., Noireaux, V., Murray, R. M., and Lucks, J. B. (2015) Rapidly characterizing the fast dynamics of RNA genetic circuitry with cell-free transcription-translation (TX-TL) systems, *ACS Synth. Biol. 4*, 503-515.
[18] Zadeh, J. N., Steenberg, C. D., Bois, J. S., Wolfe, B. R., Pierce, M. B., Khan, A. R., Dirks, R. M., and Pierce, N. A. (2011) NUPACK: Analysis and design of nucleic acid systems, *J. Comput. Chem. 32*, 170-173.
[19] Zuker, M. (2003) Mfold web server for nucleic acid folding and hybridization prediction, *Nucleic Acids Res. 31*, 3406-3415.
[20] Watters, K. E., Abbott, T. R., and Lucks, J. B. (2016) Simultaneous characterization of cellular RNA structure and function with in-cell SHAPE-Seq, *Nucleic Acids Res. 44*, e12.
[21] Sowa, S. W., Vazquez-Anderson, J., Clark, C. A., De La Pena, R., Dunn, K., Fung, E. K., Khoury, M. J., and Contreras, L. M. (2015) Exploiting post-transcriptional regulation to probe RNA structures in vivo via fluorescence, *Nucleic Acids Res. 43*, e13.
[22] Na, D., Yoo, S. M., Chung, H., Park, H., Park, J. H., and Lee, S. Y. (2013) Metabolic engineering of *Escherichia coli* using synthetic small regulatory RNAs, *Nat. Biotechnol. 31*, 170-174.
[23] Desai, R. P., and Papoutsakis, E. T. (1999) Antisense RNA strategies for metabolic engineering of *Clostridium acetobutylicum*, *Appl. Environ. Microbiol. 65*, 936-945.
[24] Stevens, J. T., and Carothers, J. M. (2015) Designing RNA-Based Genetic Control Systems for Efficient Production from Engineered Metabolic Pathways, *ACS Synth. Biol. 4*, 107-115.
[25] Green, A. A., Kim, J., Ma, D., Silver, P. A., Collins, J. J., and Yin, P. (2017) Complex cellular logic computation using ribocomputing devices, *Nature 548*, 117-121.
[26] Rodrigo, G., Landrain, T. E., and Jaramillo, A. (2012) De novo automated design of small RNA circuits for engineering synthetic riboregulation in living cells, *Proc. Natl. Acad. Sci. U.S.A. 109*, 15271-15276.
[27] Porter, E. B., Polaski, J. T., Morck, M. M., and Batey, R. T. (2017) Recurrent RNA motifs as scaffolds for genetically encodable small-molecule biosensors, *Nat. Chem. Biol. 13*, 295-301.
[28] Nissim, L., Perli, S. D., Fridkin, A., Perez-Pinera, P., and Lu, T. K. (2014) Multiplexed and programmable regulation of gene networks with an integrated RNA and CRISPR/Cas toolkit in human cells, *Mol. Cell 54*, 698-710.
[29] Qi, L. S., and Arkin, A. P. (2014) A versatile framework for microbial engineering using synthetic non-coding RNAs, *Nat. Rev. Microbiol. 12*, 341-354.
[30] Meyer, S., Chappell, J., Sankar, S., Chew, R., and Lucks, J. B. (2016) Improving fold activation of small transcription activating RNAs (STARs) with rational RNA engineering strategies, *Biotechnol. Bioeng. 113*, 216-225.
[31] Westbrook, A. M., and Lucks, J. B. (2017) Achieving large dynamic range control of gene expression with a compact RNA transcription-translation regulator, *Nucleic Acids Res. 45*, 5614-5624.
[32] Moller, T., Franch, T., Hojrup, P., Keene, D. R., Bachinger, H. P., Brennan, R. G., and Valentin-Hansen, P. (2002) Hfq: a bacterial Sm-like protein that mediates RNA-RNA interaction, *Mol. Cell 9*, 23-30.
[33] Zhang, A., Wassarman, K. M., Rosenow, C., Tjaden, B. C., Storz, G., and Gottesman, S. (2003) Global analysis of small RNA and mRNA targets of Hfq, *Mol. Microbiol. 50*, 1111-1124.
[34] Man, S., Cheng, R., Miao, C., Gong, Q., Gu, Y., Lu, X., Han, F., and Yu, W. (2011) Artificial trans-encoded small non-coding RNAs specifically silence the selected gene expression in bacteria, *Nucleic Acids Res. 39*, e50.
[35] De Lay, N., Schu, D. J., and Gottesman, S. (2013) Bacterial small RNA-based negative regulation: Hfq and its accomplices, *J. Biol. Chem. 288*, 7996-8003.

[36] Sakai, Y., Abe, K., Nakashima, S., Yoshida, W., Ferri, S., Sode, K., and Ikebukuro, K. (2014) Improving the gene-regulation ability of small RNAs by scaffold engineering in *Escherichia coli*, *ACS Synth. Biol. 3*, 152-162.
[37] Sagawa, S., Shin, J. E., Hussein, R., and Lim, H. N. (2015) Paradoxical suppression of small RNA activity at high Hfq concentrations due to random-order binding, *Nucleic Acids Res. 43*, 8502-8515.
[38] Kittleson, J. T., Cheung, S., and Anderson, J. C. (2011) Rapid optimization of gene dosage in *E. coli* using DIAL strains, *J. Biol. Eng. 5*, 10.
[39] Brantl, S. (2007) Regulatory mechanisms employed by cis-encoded antisense RNAs, *Curr. Opin. Microbiol. 10*, 102-109.
[40] Sharma, V., Yamamura, A., and Yokobayashi, Y. (2012) Engineering Artificial Small RNAs for Conditional Gene Silencing in Escherichia coli, *Acs Synthetic Biology 1*, 6-13.
[41] Kingsford, C. L., Ayanbule, K., and Salzberg, S. L. (2007) Rapid, accurate, computational discovery of Rho-independent transcription terminators illuminates their relationship to DNA uptake, *Genome Biol. 8*, R22.
[42] Bonnet, J., Yin, P., Ortiz, M. E., Subsoontorn, P., and Endy, D. (2013) Amplifying genetic logic gates, *Science 340*, 599-603.
[43] Peters, J. M., Vangeloff, A. D., and Landick, R. (2011) Bacterial transcription terminators: the RNA 3'-end chronicles, *J. Mol. Biol. 412*, 793-813.
[44] Chen, Y. J., Liu, P., Nielsen, A. A., Brophy, J. A., Clancy, K., Peterson, T., and Voigt, C. A. (2013) Characterization of 582 natural and synthetic terminators and quantification of their design constraints, *Nat. Methods 10*, 659-664.
[45] Hoynes-O'Connor, A., Hinman, K., Kirchner, L., and Moon, T. S. (2015) De novo design of heat-repressible RNA thermosensors in *E. coli*, *Nucleic Acids Res. 43*, 6166-6179.
[46] Huang, L. F., Yuan, Z. J., Liu, P. J., and Zhou, T. S. (2015) Effects of promoter leakage on dynamics of gene expression, *BMC Syst. Biol. 9*, 16.
[47] Datsenko, K. A., and Wanner, B. L. (2000) One-step inactivation of chromosomal genes in *Escherichia coli* K-12 using PCR products, *Proc. Natl. Acad. Sci. U.S.A. 97*, 6640-6645.
[48] Thomason, M. K., and Storz, G. (2010) Bacterial Antisense RNAs: How Many Are There, and What Are They Doing?, *Annu. Rev. Genet. 44*, 167-188.
[49] Storz, G., Vogel, J., and Wassarman, K. M. (2011) Regulation by small RNAs in bacteria: expanding frontiers, *Mol. Cell 43*, 880-891.
[50] Desnoyers, G., Bouchard, M. P., and Masse, E. (2013) New insights into small RNA-dependent translational regulation in prokaryotes, *Trends Genet. 29*, 92-98.
[51] Beisel, C. L., and Smolke, C. D. (2009) Design Principles for Riboswitch Function, *PLoS Comput. Biol. 5*, e1000363.
[52] Qi, L., Lucks, J. B., Liu, C. C., Mutalik, V. K., and Arkin, A. P. (2012) Engineering naturally occurring trans-acting non-coding RNAs to sense molecular signals, *Nucleic Acids Res. 40*, 5775-5786.
[53] Morra, R., Shankar, J., Robinson, C. J., Halliwell, S., Butler, L., Upton, M., Hay, S., Micklefield, J., and Dixon, N. (2016) Dual transcriptional-translational cascade permits cellular level tuneable expression control, *Nucleic Acids Res. 44*, e21.
[54] Liu, C. C., Qi, L., Lucks, J. B., Segall-Shapiro, T. H., Wang, D., Mutalik, V. K., and Arkin, A. P. (2012) An adaptor from translational to transcriptional control enables predictable assembly of complex regulation, *Nature Methods 9*, 1088-1094.
[55] Dueber, J. E., Wu, G. C., Malmirchegini, G. R., Moon, T. S., Petzold, C. J., Ullal, A. V., Prather, K. L., and Keasling, J. D. (2009) Synthetic protein scaffolds provide modular control over metabolic flux, *Nat. Biotechnol. 27*, 753-759.
[56] Paradise, E. M., Kirby, J., Chan, R., and Keasling, J. D. (2008) Redirection of flux through the FPP branch-point in *Saccharomyces cerevisiae* by down-regulating squalene synthase, *Biotechnol. Bioeng. 100*, 371-378.
[57] Smolke, C. D., Martin, V. J. J., and Keasling, J. D. (2001) Controlling the metabolic flux through the carotenoid pathway using directed mRNA processing and stabilization, *Metab. Eng. 3*, 313-321.

[58] Andersen, J. B., Sternberg, C., Poulsen, L. K., Bjorn, S. P., Givskov, M., and Molin, S. (1998) New unstable variants of green fluorescent protein for studies of transient gene expression in bacteria, *Appl. Environ. Microbiol. 64*, 2240-2246.
[59] Gardner, T. S., Cantor, C. R., and Collins, J. J. (2000) Construction of a genetic toggle switch in Escherichia coli, *Nature 403*, 339-342.
[60] Elowitz, M. B., and Leibler, S. (2000) A synthetic oscillatory network of transcriptional regulators, *Nature 403*, 335-338.
[61] Moon, T. S., Lou, C. B., Tamsir, A., Stanton, B. C., and Voigt, C. A. (2012) Genetic programs constructed from layered logic gates in single cells, *Nature 491*, 249-253.
[62] Shopera, T., Henson, W. R., and Moon, T. S. (2017) Dynamics of sequestration-based gene regulatory cascades, *Nucleic Acids Res. 45*, 7515-7526.
[63] Stanton, B. C., Nielsen, A. A. K., Tamsir, A., Clancy, K., Peterson, T., and Voigt, C. A. (2014) Genomic mining of prokaryotic repressors for orthogonal logic gates, *Nat. Chem. Biol. 10*, 99-105.
[64] Khalil, A. S., and Collins, J. J. (2010) Synthetic biology: applications come of age, *Nature reviews 11*, 367-379.
[65] Larson, M. H., Gilbert, L. A., Wang, X. W., Lim, W. A., Weissman, J. S., and Qi, L. S. (2013) CRISPR interference (CRISPRi) for sequence-specific control of gene expression, *Nat. Protoc. 8*, 2180-2196.
[66] Townshend, B., Kennedy, A. B., Xiang, J. S., and Smolke, C. D. (2015) High-throughput cellular RNA device engineering, *Nat. Methods 12*, 989-994.
[67] Callura, J. M., Dwyer, D. J., Isaacs, F. J., Cantor, C. R., and Collins, J. J. (2010) Tracking, tuning, and terminating microbial physiology using synthetic riboregulators, *Proc. Natl. Acad. Sci. U.S.A. 107*, 15898-15903.
[68] Durfee, T., Nelson, R., Baldwin, S., Plunkett, G., 3rd, Burland, V., Mau, B., Petrosino, J. F., Qin, X., Muzny, D. M., Ayele, M., Gibbs, R. A., Csorgo, B., Posfai, G., Weinstock, G. M., and Blattner, F. R. (2008) The complete genome sequence of *Escherichia coli* DH10B: insights into the biology of a laboratory workhorse, *J .Bacteriol. 190*, 2597-2606.
[69] Engler, C., Kandzia, R., and Marillonnet, S. (2008) A one pot, one step, precision cloning method with high throughput capability, *PloS one 3*, e3647.

FIGURES AND FIGURE CAPTIONS

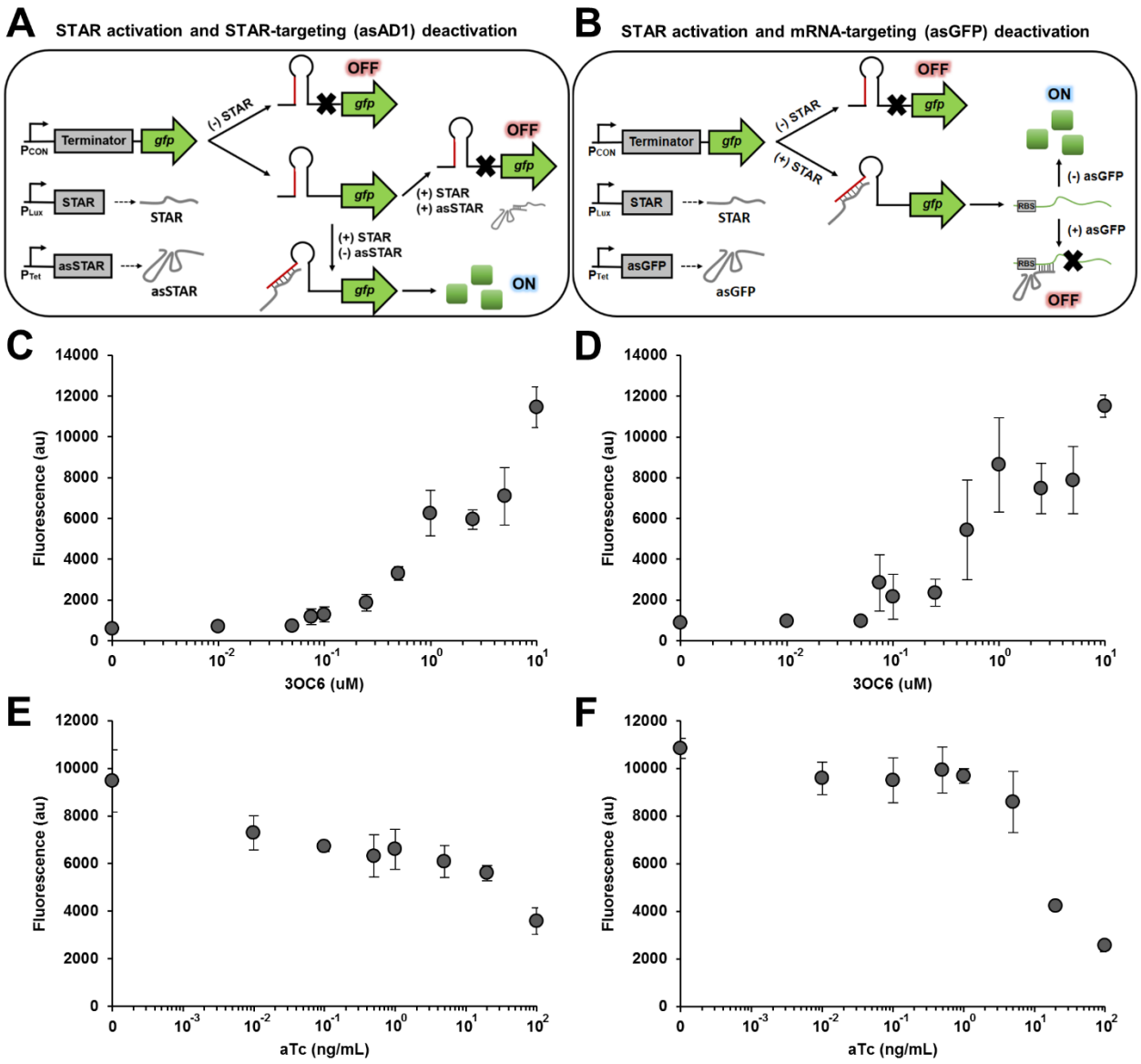

Figure 1. Multilevel regulation of gene expression with the combined STAR and asRNA system. (A, B) Genetic circuits built by combining the STAR system with asRNA. A STAR regulator activates GFP expression by disrupting the hairpin formation of STAR-target. GFP is 'on' when the STAR regulator is present (denoted by +) in the absence of asRNA (asSTAR or asGFP), and GFP is 'off' when the STAR regulator is absent (denoted by -). STAR regulators are transcribed by the 3OC6-inducible P_{Lux} promoter. The GFP expression is deactivated when an asSTAR binds to its target STAR regulator (A), or when an asGFP binds to its target *gfpmut3* mRNA (B). Both asSTAR and asGFP are transcribed by the aTc-inducible P_{Tet} promoter. **(C, D)** Activation of GFP expression was tested by varying the AD1.A5 STAR regulator expression level in the STAR-targeting system (C) and the mRNA-targeting system (D). *gfpmut3* is under the

control of the constitutive Bba_J23119 promoter and the AD1.S5 STAR-target.[10] Cells were grown in the presence of different 3OC6 concentrations (0, 0.01, 0.05, 0.075, 0.1, 0.25, 0.5, 1, 2.5, 5, and 10 μM). **(E, F)** Deactivation of GFP expression was tested by varying the asAD1.A5 (E) or asGFP1 (F) expression level. Cells were grown in the presence of 5 μM 3OC6 with different aTc concentrations (0, 0.01, 0.1, 0.5, 1, 5, 20, and 100 ng/mL). The fluorescence (au) is reported by calculating $[(F_{experimental}/Abs_{experimental}) - (F_{negative\ control}/Abs_{negative\ control})]$, where the negative control is the JTK165JK strain without a plasmid (see Supplementary Figure S4 for the fluorescence values of JTK165JK strains with or without blank plasmids, which were statistically indistinguishable). F is the measured fluorescence (excitation at 483 nm and emission at 530 nm), and Abs is the measured absorbance at 600 nm. The fluorescence (au) was measured using a microplate reader. See Supplementary Figure S2 for the absorbance at 600 nm. The error bars represent the standard deviation of the fluorescence values from three biological replicates performed on different days.

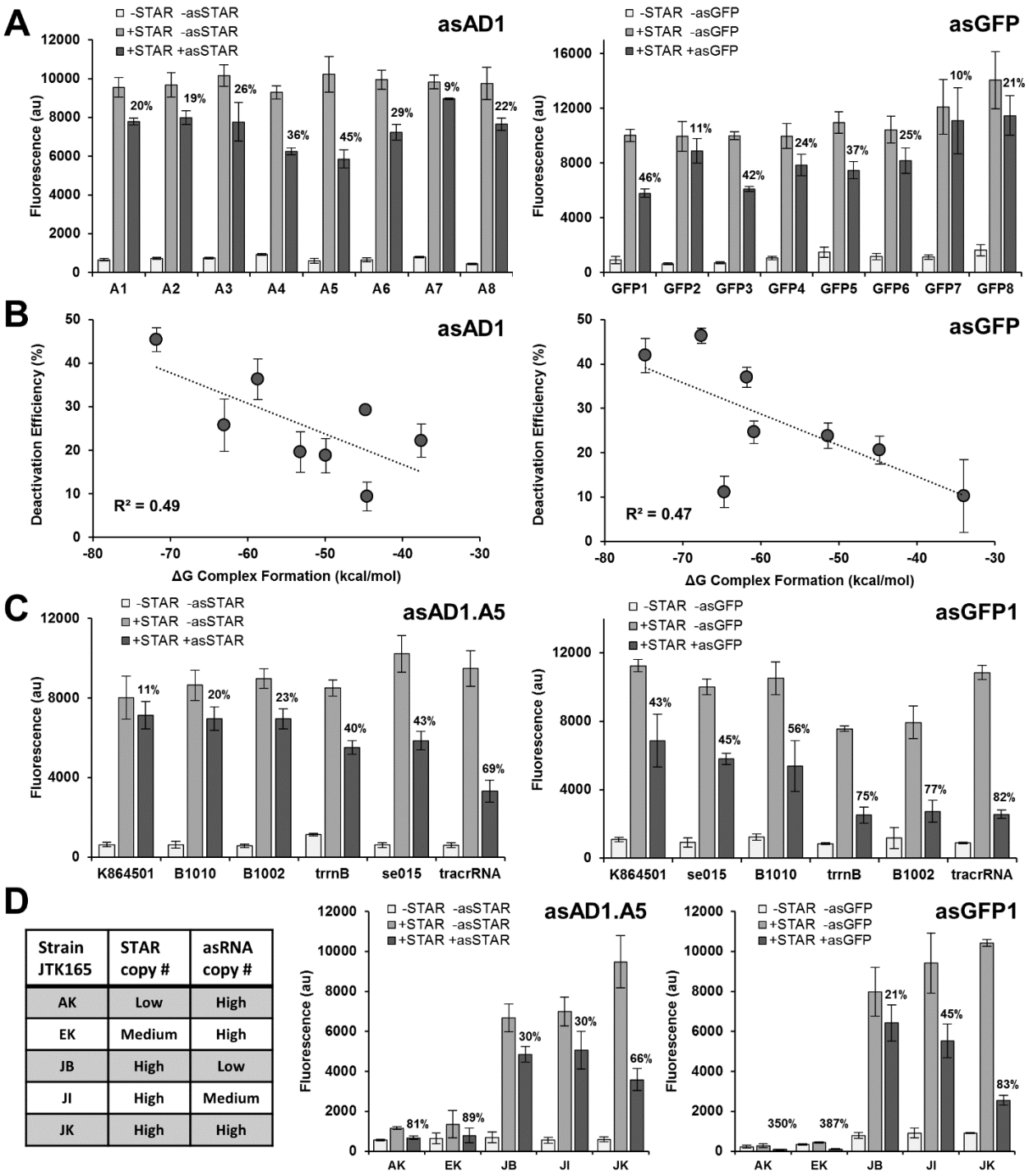

Figure 2. Improvement in deactivation efficiency by changing genetic elements. (A) Deactivation of GFP expression by either asAD1 (asSTAR) or asGFP variants that have different ΔG Complex Formation values (see (B) for the correlation; Supplementary Figure S7 for the values and the target region). The target region was restricted to 68 nucleotides of the AD1.A5 STAR regulator, or 80 nucleotides containing the RBS of *gfpmut3* mRNA (-16 to +64 with the start codon's A as +1). The transcription of asSTAR and asGFP variants was terminated by the se015

terminator. Bba_J23119 promoter (http://parts.igem.org/Promoters/Catalog/Anderson) was used to transcribe *gfpmut3* in the reporter plasmid (ColE1 origin, high copy number). Cells were grown in the presence of 5 μM 3OC6 to activate GFP expression, and 5 μM 3OC6 and 100 ng/mL aTc to deactivate GFP expression. Deactivation efficiencies are indicated on the graph. Deactivation efficiency was calculated by $[(F_{STAR}/Abs_{STAR} - F_{STAR,asRNA}/Abs_{STAR,asRNA}) / (F_{STAR}/Abs_{STAR} - F_{negative\ control}/Abs_{negative\ control})] \times 100\%$, where the negative control is JTK165JK with both STAR and asRNA systems uninduced. The subscript indicates induced systems. **(B)** A moderate negative correlation was observed between ΔG Complex Formation of asSTAR-AD1.A5 complex or asGFP-*gfpmut3* mRNA complex and deactivation efficiency (R^2 = 0.49 and 0.47, $p < 0.01$). **(C)** Increase or decrease in deactivation efficiencies due to different transcription terminators on the 3'-end of asAD1.A5 and asGFP1. asAD1.A5 and asGFP1, which showed the highest deactivation efficiency in (A), were selected and tested with different transcription terminators (See Supplementary Table 2 for sequences). Cells were grown in the presence of 5 μM 3OC6 to activate GFP expression, and 5 μM 3OC6 and 100 ng/mL aTc to deactivate GFP expression. Deactivation efficiencies are indicated on the graph. **(D)** Effect of changing plasmid copy numbers on deactivation efficiency. Various JTK165 DIAL strains (AK, EK, JB, JI, and JK) with different plasmid copy numbers were used to vary the ratio of the AD1.A5 STAR regulator to asAD1.A5 or asGFP1. The first letter indicates the copy number of R6K origin, and the second letter indicates the copy number of ColE2 origin. The alphabet denotes the copy number in the order of low (A or B), medium (E or I), and high (J or K). The AD1.A5 STAR regulator and asAD1.A5 or asGFP1 were transcribed from the plasmids with R6K and ColE2 origins, respectively. Cells were grown in the presence of 5 μM 3OC6 to activate GFP expression, and 5 μM 3OC6 and 100 ng/mL aTc to deactivate GFP expression. Deactivation efficiencies are indicated on the graph. The fluorescence (au) was reported by calculating $[(F_{experimental}/Abs_{experimental}) - (F_{negative\ control}/Abs_{negative\ control})]$, where the negative control is the JTK165JK strain without a plasmid. F is the measured fluorescence (excitation at 483 nm and emission at 530 nm), and Abs is the measured absorbance at 600 nm. The fluorescence (au) was measured using a microplate reader. The error bars represent the standard deviation of the fluorescence values from three biological replicates performed on different days.

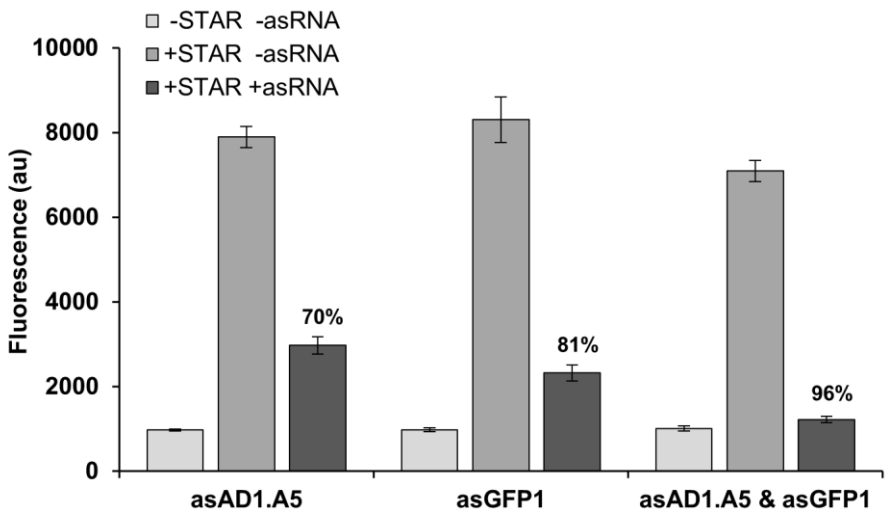

Figure 3. Improved deactivation efficiency by integrating the two types of asRNAs. The deactivation efficiency can be improved by expressing both asAD1.A5 (asSTAR) and asGFP1 (asGFP) that target the AD1.A5 STAR regulator and *gfpmut3* mRNA, respectively. A significant difference in deactivation was observed between cells expressing asAD1.A5 and cells expressing both asAD1.A5 and asGFP1, determined by two-sample *t*-test (t = -10.11, $p < 0.01$). A significant difference in deactivation was also observed between cells expressing asGFP1 and cells expressing both asAD1.A5 and asGFP1, determined by two-sample *t*-test (t = -5.18, $p < 0.01$). *gfpmut3* is under the control of the constitutive Bba_J23119 promoter and the AD1.S5 STAR-target.[10] The AD1.A5 STAR regulator was transcribed by the 3OC6-inducible P_{Lux} promoter. Both asAD1.A5 and asGFP1 were transcribed by the aTc-inducible P_{Tet} promoters. Cells were grown in the presence of 5 μM 3OC6 to activate GFP expression, and 5 μM 3OC6 and 100 ng/mL aTc to deactivate GFP expression. Deactivation efficiencies are indicated on the graph. The fluorescence (au) was reported by calculating $[(F_{experimental}/Abs_{experimental}) - (F_{negative\ control}/Abs_{negative\ control})]$, where the negative control is the JTK165JK strain without a plasmid. F is the measured fluorescence (excitation at 483 nm and emission at 530 nm), and Abs is the measured absorbance at 600 nm. Deactivation efficiency was calculated by $[(F_{STAR}/Abs_{STAR} - F_{STAR,asRNA}/Abs_{STAR,asRNA}) / (F_{STAR}/Abs_{STAR} - F_{negative\ control}/Abs_{negative\ control})] \times 100\%$, where the negative control is JTK165JK with both STAR and asRNA systems uninduced. The fluorescence (au) was measured using a microplate reader. The error bars represent the standard deviation of the fluorescence values from three biological replicates performed on different days.

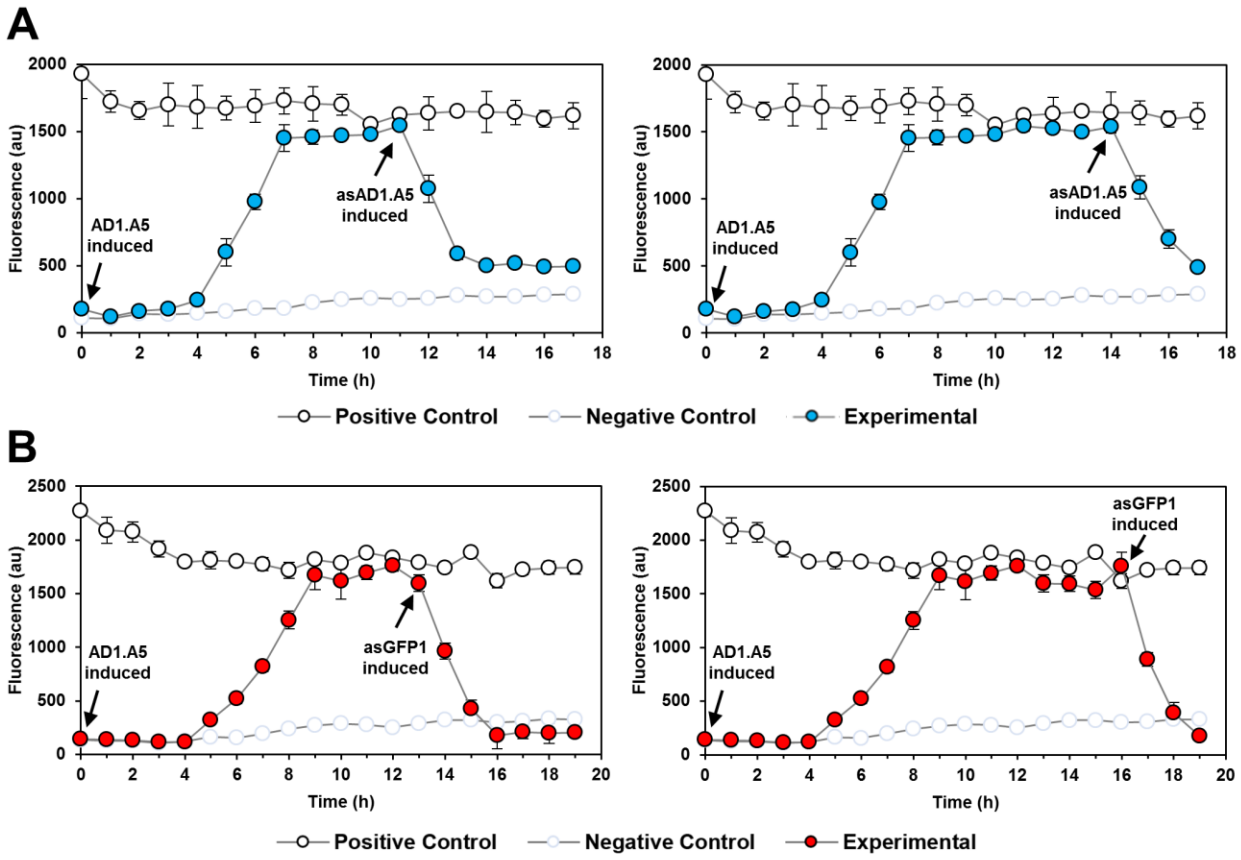

Figure 4. Real-time control of GFP expression using the combined STAR and asRNA system. Activation of GFP expression was first achieved by inducing the STAR system only in cells that contain both the AD1.A5 STAR regulator (induced) and asAD1.A5 (uninduced) (A), or both the AD1.A5 STAR regulator (induced) and asGFP1 (uninduced) (B). Cells with the absorbance of 0.01 were induced with 5 μM 3OC6 at t = 0 h (see Figures 1A and 1B for the schematic figures). **(A)** A significant activation was observed by 4 h, determined by two-sample *t*-test ($t = 4.63$, $p < 0.05$).[16] At t = 11 h (left) and 14 h (right), cells were transferred into fresh media (diluted back to Abs=0.01), and both STAR and asSTAR systems were activated (induced with 5 μM 3OC6 and 100 ng/mL aTc). A significant deactivation was observed by 1 h after the transfer, determined by two-sample *t*-test ($t = 10.68$, $p < 0.01$).[16] Response times (1 h) were independent of the duration of the activation (11 or 14 h). Negative controls are cells without inducers and positive controls are cells with the STAR system activated only (induced with 5 μM 3OC6). **(B)** A significant activation was observed by 5 h, determined by two-sample *t*-test ($t = 2.78$, $p < 0.01$).[16] At t = 13 h (left) and 16 h (right), cells were transferred into fresh media (diluted back to Abs=0.01), and both STAR and asGFP systems were activated (induced with 5 μM 3OC6 and 100 ng/mL aTc). A significant deactivation was observed by 1 h after the transfer, determined by two-sample *t*-test ($t = 2.78$, $p < 0.01$).[16] Response times (1 h) were independent of the duration of the activation (13 or 16 h). Negative controls are cells without inducers and positive controls are cells with the STAR system activated only (induced with 5 μM 3OC6). Fluorescence (au) was measured using flow cytometry, and the error bars represent the standard deviation of the fluorescence values from three biological replicates.

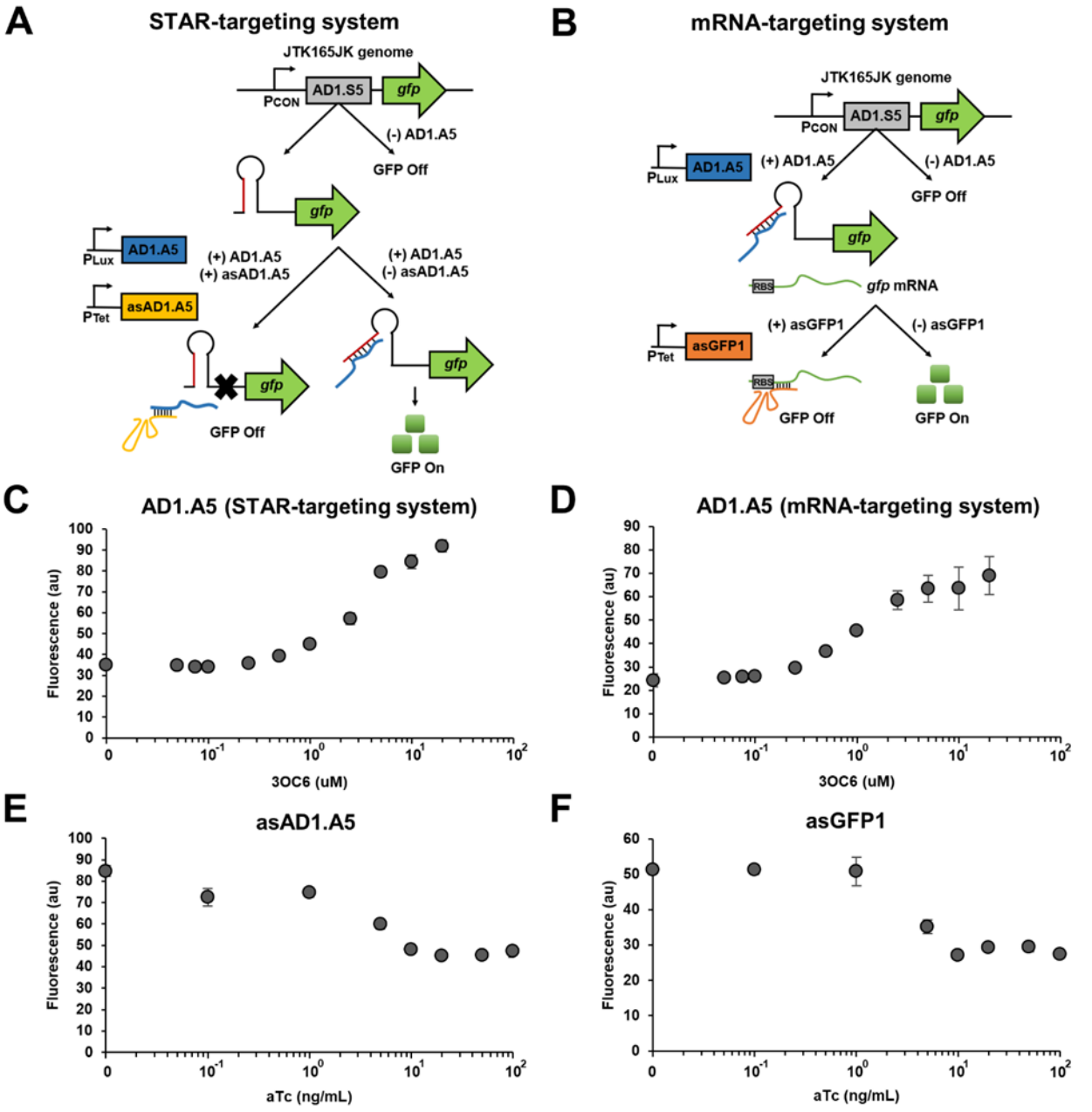

Figure 5. Characterization of the combined system targeting a gene in the genome. The AD1.S5-*gfpmut3* cassette was integrated into the JTK165JK genome using λ Red recombination (*bglA*::AD1.S5-*gfpmut3*). **(A, B)** The AD1.A5 STAR regulator activates GFP expression by binding to the AD1.S5 STAR-target that was inserted in the genome with *gfpmut3*. asAD1.A5 (A) or asGFP1 (B) deactivates GFP expression by targeting the AD1.A5 STAR regulator or *gfpmut3* mRNA, respectively. The AD1.A5 STAR regulator, asAD1.A5, and asGFP1 are transcribed from plasmids. **(C, D)** Activation of GFP expression was tested by varying the AD1.A5 STAR regulator expression level in the STAR-targeting system (C) and the mRNA-targeting system (D). Cells were grown in the presence of different 3OC6 concentrations (0, 0.05, 0.075, 0.1, 0.25, 0.5, 1, 2.5, 5, 10, and 20 μM). **(E, F)** Deactivation of GFP expression was tested by varying the asAD1.A5 (E) or asGFP1 (F) expression level. Cells were grown in the presence of 5 μM 3OC6 with different

aTc concentrations (0, 0.1, 1, 5, 10, 20, 50, and 100 ng/mL). The fluorescence (au) was reported by calculating $[(F_{experimental}/Abs_{experimental}) - (F_{negative\ control}/Abs_{negative\ control})]$, where the negative control is the wild-type JTK165JK strain without a plasmid. The fluorescence (au) was measured using a microplate reader. The error bars represent the standard deviation of the fluorescence values from three biological replicates performed on different days.

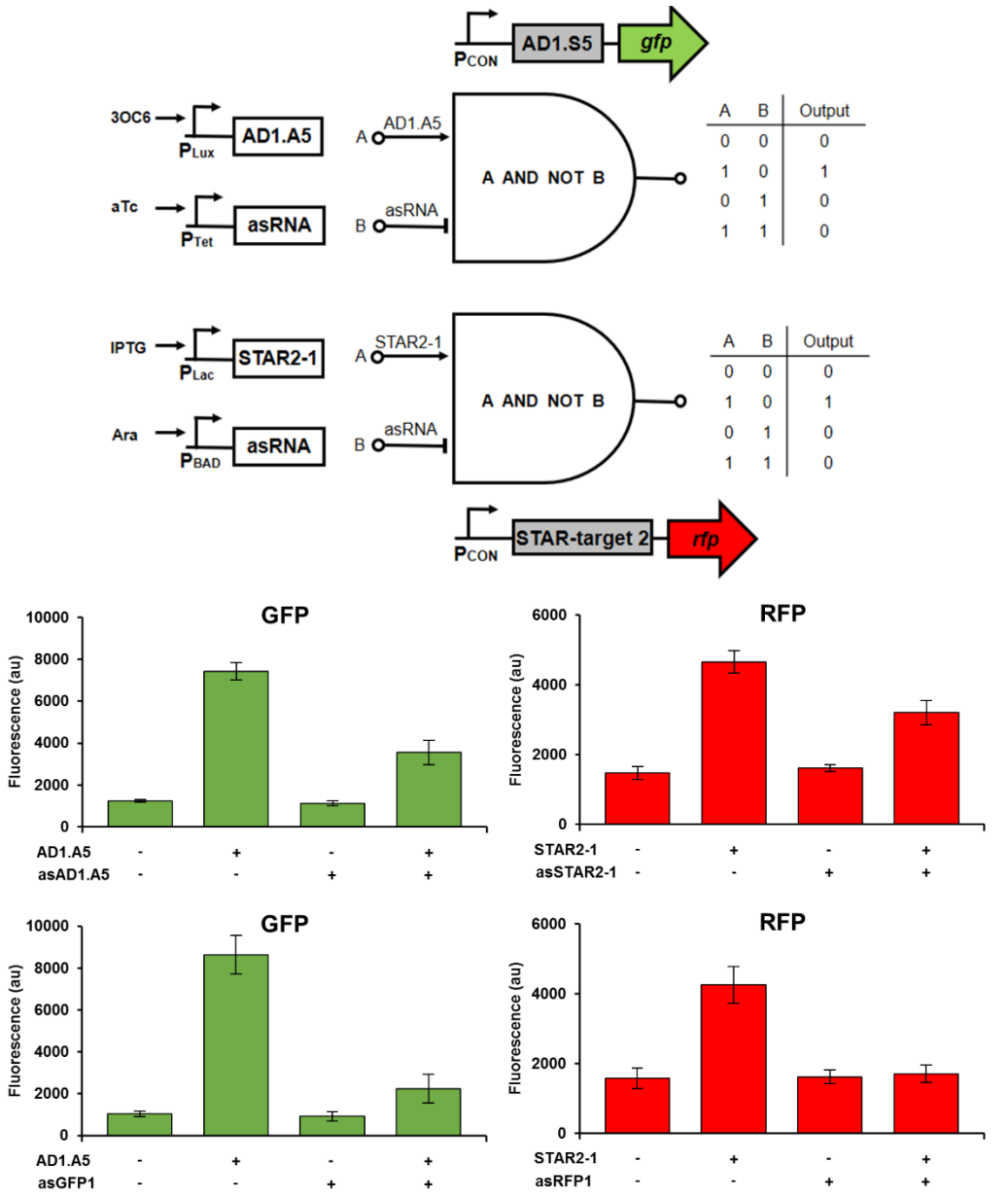

Figure 6. Multiplexing with the combined STAR and asRNA system. Two A AND NOT B logic gates (the output is 'on' only in the presence of A input and in the absence of B input) were constructed in the same cell, with each gate controlling either *gfpmut3* or *rfp*. The AD1.A5 STAR regulator binds to the AD1.S5 STAR-target to activate GFP expression. The asAD1.A5 binds to the AD1.A5 STAR regulator, and the asGFP1 binds to the *gfpmut3* mRNA to deactivate GFP expression. The STAR2-1 STAR regulator binds to the STAR-target 2 to activate RFP expression. The asSTAR2-1 binds to the STAR2-1 STAR regulator, and the asRFP1 binds to the *rfp* mRNA to deactivate RFP expression. AD1.A5 and STAR2-1 were transcribed by the 3OC6-inducible P_{Lux} and IPTG-inducible P_{Lac} promoters, respectively. asAD1.A5 or asGFP1 was transcribed by the aTc-inducible P_{Tet} promoter. asSTAR2-1 or asRFP1 was transcribed by the Ara-inducible P_{BAD} promoter. Each RNA regulator specifically activated or deactivated its cognate gene, but not the

other gene. See Supplementary Figure S10 for the orthogonality of STAR regulators (AD1.A5 and STAR2-1) and asRNAs (asAD1.A5, asSTAR2-1, asGFP1, and asRFP1). The cells were grown in the presence of either 5 μM 3OC6 (+ for AD1.A5) or 20 mM IPTG (+ for STAR2-1), and either 100 ng/mL aTc (+ for asAD1.A5 or asGFP1) or 40 mM Ara (+ for asSTAR2-1 or asRFP1). + and - indicate induced and uninduced systems. *gfpmut3* and *rfp* are under the control of the constitutive Bba_J23119 and Bba_J23105 promoters, respectively. The fluorescence (au) was reported by calculating $[(F_{experimental}/Abs_{experimental}) - (F_{negative\ control}/Abs_{negative\ control})]$, where the negative control is the JTK165JK strain without a plasmid. The fluorescence (au) was measured using a microplate reader. GFP was measured with excitation at 483 nm and emission at 530 nm, and RFP was measured with excitation at 535 nm and emission at 620 nm. The error bars represent the standard deviation of the fluorescence values from three biological replicates performed on different days.

Graphical Table of Contents